

## Catalytic activities of CuO/TiO<sub>2</sub> and CuO-ZrO<sub>2</sub>/TiO<sub>2</sub> in NO + CO reaction

Jiang Xiaoyuan<sup>a,\*</sup>, Ding Guanghui<sup>a</sup>, Lou Liping<sup>b</sup>, Chen Yingxu<sup>b</sup>, Zheng Xiaoming<sup>a</sup>

<sup>a</sup> Institute of Catalysis, Faculty of Science, Zhejiang University, Hangzhou 310028, PR China

<sup>b</sup> Institute of Environmental Engineering, Faculty of Environment and Resource, Zhejiang University, Hangzhou 310029, PR China

Received 2 October 2003; received in revised form 14 December 2003; accepted 20 February 2004

### Abstract

CuO/TiO<sub>2</sub> and CuO-ZrO<sub>2</sub>/TiO<sub>2</sub> catalysts with different CuO loadings were prepared by the impregnation method using Cu(NO<sub>3</sub>)<sub>2</sub> and Ce(NO<sub>3</sub>)<sub>3</sub> aqueous solutions of desired concentrations. The catalytic activities in NO + CO reaction were investigated, and the structural and reductive properties of various CuO/TiO<sub>2</sub> and CuO-ZrO<sub>2</sub>/TiO<sub>2</sub> catalysts were characterized by means of BET, TPR, XRD and NO-TPD technology. It was found that after treatment in H<sub>2</sub> at 500 °C for 2 h, the catalytic activities were improved dramatically compared with treatment in normal air at 500 °C for 2 h. The NO conversion temperature ( $T_{99\%}$ ) was 325 °C for 6% CuO/TiO<sub>2</sub> and 300 °C for 6% CuO-10% ZrO<sub>2</sub>/TiO<sub>2</sub>, and their activities increased with increase in ZrO<sub>2</sub> loading. There were four TPR peaks in CuO/TiO<sub>2</sub> and two TPR peaks in CuO-ZrO<sub>2</sub>/TiO<sub>2</sub>, indicating that addition of ZrO<sub>2</sub> caused changes in CuO species on TiO<sub>2</sub>. The air-treated catalysts displayed CuO diffraction peaks, whereas the H<sub>2</sub>-treated catalysts displayed Cu metal diffraction peaks. Four desorption species (NO, N<sub>2</sub>O, N<sub>2</sub> and O<sub>2</sub>) were detected during the thermal desorption of NO by CuO/TiO<sub>2</sub> and CuO-ZrO<sub>2</sub>/TiO<sub>2</sub> treated in both air and H<sub>2</sub>. There were two adsorption states of nitric oxide (NO) on the catalyst's surface, i.e. desorption species at low temperature on the weak sites and at high temperature on the strong sites. Addition of ZrO<sub>2</sub> onto CuO/TiO<sub>2</sub> shifted the NO dissociation peaks towards low temperature, which means that the activity of NO decomposition was higher by CuO-ZrO<sub>2</sub>/TiO<sub>2</sub> than by CuO/TiO<sub>2</sub>. The NO + CO reaction formed intermediary product N<sub>2</sub>O at low temperature but formed N<sub>2</sub> at high temperature. In addition, the peak temperature of NO desorption corresponded with the catalyst's activity under both air and H<sub>2</sub>, and the dissociation of NO on catalyst surface was a rate-determining step in NO + CO reaction.

© 2004 Elsevier B.V. All rights reserved.

**Keywords:** CuO/TiO<sub>2</sub> and CuO-ZrO<sub>2</sub>/TiO<sub>2</sub> catalysts; NO + CO reaction; NO-TPD

### 1. Introduction

Nitric oxide (NO) is one of the major air pollutants particularly in the modern large cities. It is estimated that 35–38 × 10<sup>6</sup> tonnes of NO are released from the exhaust gases of automobiles every year in the world. NO causes severe environmental hazards and is very harmful to the health of human being. The common methods of NO treatment include liquid or solid absorption, selective catalytic reduction of NO with NH<sub>3</sub> and electronic irradiation. However, all these methods result in incomplete NO treatment and cause secondary pollutions. Since 1980s, scientists have been looking for highly efficient DeNO<sub>x</sub> catalysts to eliminate NO through reductive mechanism. In early 1989,

Iwamoto et al. [1,2] found that Cu-ZSM5 catalyst had much better catalytic activity for NO dissociation. Since then, catalytic reduction of NO has been extensively studied and variety of transition and noble metal catalysts were prepared [3,4]. In recent years, use of TiO<sub>2</sub> as catalyst's carrier has attracted much attention and TiO<sub>2</sub>-based catalysts are widely applied in NO reduction [5–8]. TiO<sub>2</sub>-based catalysts overcome the shortcoming of TiO<sub>2</sub> and SO<sub>x</sub> interaction that produces sulphate and causes structural collapse of the carrier, particle gathering of active components and reduction of active surfaces. As a result, the catalytic reduction of NO can be achieved in a sulphur-containing atmosphere, and obtain an excellent NO conversion and N<sub>2</sub> selectivity.

Various physicochemical methods are also used to investigate the state of copper ion in CuO/TiO<sub>2</sub> catalysts, and inconsistent results have been reported. Komova et al. [7] found that TiO<sub>2</sub>-supported CuO could exist as Cu<sup>2+</sup> ions,

\* Corresponding author. Tel.: +86-571-88273272.

E-mail address: [xyjiang@mail.hz.zj.cn](mailto:xyjiang@mail.hz.zj.cn) (J. Xiaoyuan).

bulk CuO, chain stabilized  $\text{Cu}^{2+}$  ions, and two different oxide clusters with a structure similar to CuO. In contrast, Xu et al. [8] reported two  $\text{Cu}^{2+}$  ions with significantly different reducibility on the anatase surface—CuO phase and highly-dispersed  $\text{Cu}^{2+}$ , similar to  $\text{CuO}/\gamma\text{-Al}_2\text{O}_3$ . Larsson et al. [9,10] suggested that low temperature peak in  $\text{Cu}_3\text{-Ti}$  of the  $\text{H}_2$ -TPR profiles was monomeric copper containing  $\text{Cu}^+$ , and that in  $\text{Cu}_{12}\text{-Ti}$  was polymeric copper containing  $\text{Cu}^{2+}$ . They also found that catalysts using  $\text{TiO}_2$  as carrier displayed a high catalysis in CO oxidation, and that CuO catalyst had much higher activity than  $\text{MoO}_x$ ,  $\text{FeO}_x$  and  $\text{CoO}_x$  catalysts and its activity at low temperature was even superior to  $\text{Pt}/\gamma\text{-Al}_2\text{O}_3$  catalyst.

In this study, reducibility and characteristics of the catalysts were investigated using the methods of BET, TPR, XRD and NO-TPD.  $\text{ZrO}_2$  was added onto  $\text{CuO}/\text{TiO}_2$  to examine the catalyst's activity and stability in NO + CO reaction.

## 2. Experimental

### 2.1. $\text{TiO}_2$ preparation

$\text{TiO}_2$  was prepared by sol-gel method from  $\text{TiCl}_4$  with ammonia solution as precipitating agent and ethanol as dispersing agent.  $\text{TiCl}_4$  of 25 ml was dissolved in 20 ml distilled water in an ice-water bath. The titanium solution was then slowly mixed with 30 ml distilled water and 20 ml ethanol, and ammonia was added dropwise until  $\text{pH} = 9$ . During ammoniac addition an intensive precipitation occurred. After the solvent was evaporated at  $80^\circ\text{C}$  for 24 h, the precipitates were dried at  $300^\circ\text{C}$  for 2 h to remove  $\text{NH}_4\text{Cl}$ , and then calcined in an air stream of  $450^\circ\text{C}$  for 4 h.

### 2.2. Catalyst preparation

The  $\text{CuO}/\text{TiO}_2$  and  $\text{CuO-ZrO}_2/\text{TiO}_2$  catalysts were prepared by the impregnation method using  $\text{Cu}(\text{NO}_3)_2$  and  $\text{Zr}(\text{NO}_3)_4$  aqueous solutions of desired concentrations. These catalysts were dried at  $120^\circ\text{C}$  for 2 h, followed by calcinations in an air stream of  $500^\circ\text{C}$  for 2 h. They were denoted as  $w\%$   $\text{CuO}/\text{TiO}_2$  and  $w\%$   $\text{CuO-w}'\%$   $\text{ZrO}_2/\text{TiO}_2$ , where  $w$  and  $w'$  are the amount of CuO and  $\text{ZrO}_2$  loading, respectively.

### 2.3. Measurements of catalytic characters

The BET surface area of catalysts was determined by  $\text{N}_2$  adsorption at 77 K using a Coulter OMNISORP-100 instrument.

$\text{H}_2$ -temperature programmed reduction (TPR) was done by gas chromatography (GC) using a thermal conductivity detector. The sample (5–10 mg) was activated in an  $\text{O}_2$  stream at  $500^\circ\text{C}$  for 0.5 h. After it was cooled to  $30^\circ\text{C}$ ,  $\text{H}_2$ -TPR was conducted. The reduction gas contained 5%

$\text{H}_2$  and 95% mixture of  $\text{H}_2$  and  $\text{N}_2$  at 99.999% purity. Both  $\text{H}_2$  and  $\text{N}_2$  were purified using a 401 deoxidiser and silica gel. The flow rate of the  $\text{H}_2/\text{N}_2$  mixture was  $18\text{ ml min}^{-1}$  ( $\beta = 20\text{ K min}^{-1}$ ).

X-ray diffraction (XRD) data were obtained at  $25^\circ\text{C}$  using a horizontal Rigaku B/Max III B powder diffractometer with Cu  $\text{K}\alpha$  radiation and a power of  $40 \times 30\text{ mA}$ . The diffraction angles were  $2\theta$  ( $^\circ$ ). The wavelength of the source used was Cu  $\text{K}\alpha = 1.540598\text{ \AA}$ .

To measure NO-temperature programmed desorption (TPD), 250 mg of fresh catalysts were loaded onto a quartz reactor ( $\Phi = 5\text{ mm}$ ) and reduced in  $\text{H}_2$  atmosphere at  $500^\circ\text{C}$  for 1 h, and followed by two treatments. In treatment one, catalysts were heated in He at  $600^\circ\text{C}$  for 1 h, and then cooled to  $40^\circ\text{C}$  in a flow of He and exposed to a 10% NO-He mixture gas. Excessive NO was removed, and the catalysts were kept in He flow until no significant amount of adsorbates could be detected. The catalysts were then ramped at  $600^\circ\text{C}$  at a linear heating rate of  $20^\circ\text{C min}^{-1}$  in He flow. The effluent gases were analyzed with a mass spectrometer. In treatment two, after the catalysts were heated in He at  $500^\circ\text{C}$  for 1 h, the following procedures were the same as those in treatment one.

### 2.4. Measurements of catalytic activity in NO + CO reaction

Catalytic activity was determined under the steady state in a fixed-bed quartz reactor (6 mm). The particle size of catalysts was 20–40 mesh, and 120 mg of the catalysts were used. The reaction gas (i.e. feed steam) consisted of a fixed composition of 6.0% NO, 6.0% CO and 88% He (v/v) as a dilute. The catalysts were treated using either  $\text{H}_2$  or air at  $500^\circ\text{C}$  for 1 h. After the catalysts were cooled to room temperature, they were allowed to react with the mixed gas. The reactions were operated at different temperatures at a space velocity of  $5000\text{ h}^{-1}$ . Two columns and thermal conduction detectors were used for analyzing the catalytic activity. Column A was packed with 13X molecular sieve for separating  $\text{N}_2$ , NO and CO, and Column B was packed with Porapak Q for separating  $\text{N}_2\text{O}$  and  $\text{CO}_2$  (Fig. 1). The catalytic activity was calculated using the following formula

$$[\text{NO}]_{\text{conv}} = \frac{[\text{NO}]_{\text{in}} - [\text{NO}]_{\text{out}}}{[\text{NO}]_{\text{in}}}$$

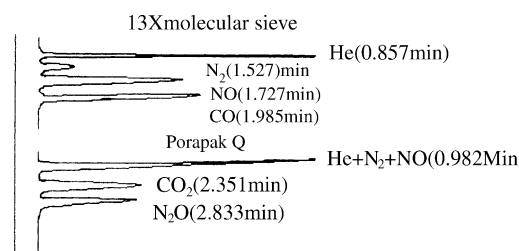


Fig. 1. Separation of reaction products by gas chromatography.

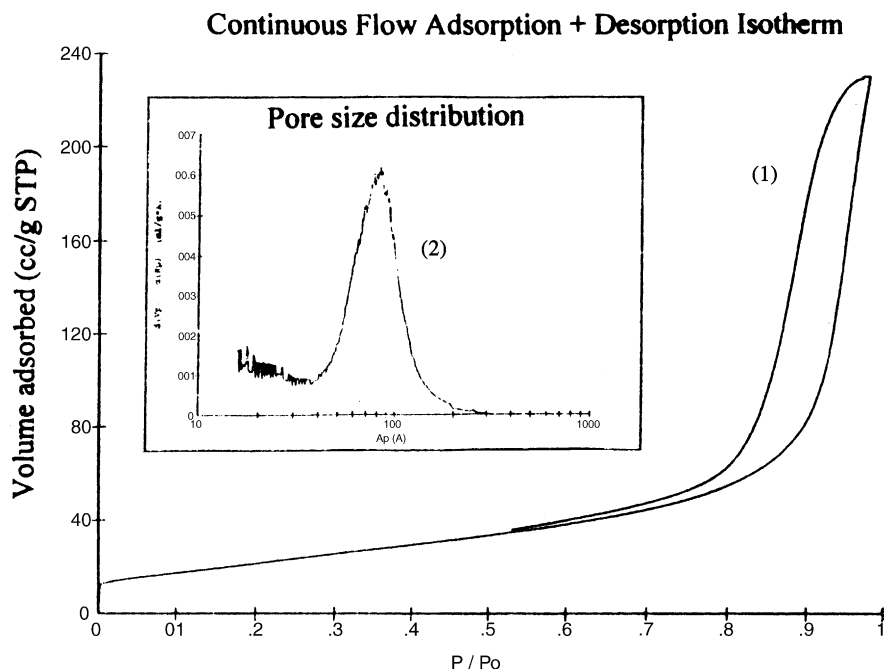


Fig. 2. Adsorption–desorption isotherm and pore-size distribution of  $\text{TiO}_2$ . (1) Adsorption–desorption isotherm. (2) Pore-size distribution.

$$[\text{N}_2]_{\text{set}} = \frac{2[\text{N}_2]}{[\text{NO}]_{\text{in}} - [\text{NO}]_{\text{out}}}$$

### 3. Results and discussion

#### 3.1. Textural and structural properties of $\text{TiO}_2$

Nitrogen adsorption–desorption by  $\text{TiO}_2$  was examined in order to estimate its specific surface area and porosity. The results showed that the material of  $\text{TiO}_2$  was porous and the  $\text{N}_2$  isotherm of  $\text{TiO}_2$  was of type IV, typical of a mesoporous sample (Fig. 2). Pore-size distribution curves calculated from the desorptive branch of the isotherm also indicated the presence of mesoporosity although they were not regularly or-

dered pores. The specific surface area and total pore volume of  $\text{TiO}_2$  were  $80.7 \text{ m}^2 \text{ g}^{-1}$  and  $3.884 \times 10^{-1} \text{ ml g}^{-1}$ . Average pore diameter and stochastic pore diameter were 19.2 and 7.0–9.0 nm, respectively.

TG-DTA analysis of  $\text{TiO}_2$  showed an absorption heat peak around  $100^\circ\text{C}$  when it was heated at a liner rate of  $20^\circ\text{C min}^{-1}$  from 50 to  $800^\circ\text{C}$ . This peak could be due to the evaporation and removal of adsorbed  $\text{H}_2\text{O}$ . An exothermic peak was also observed around  $400^\circ\text{C}$ , indicating the completion of anatase crystallization. There were no exothermic peaks above  $400^\circ\text{C}$ , suggesting that anatase transformation was a gradual process. In addition, a step of weightlessness was evident in the section of TG curve from 100 to  $250^\circ\text{C}$  (Fig. 3).

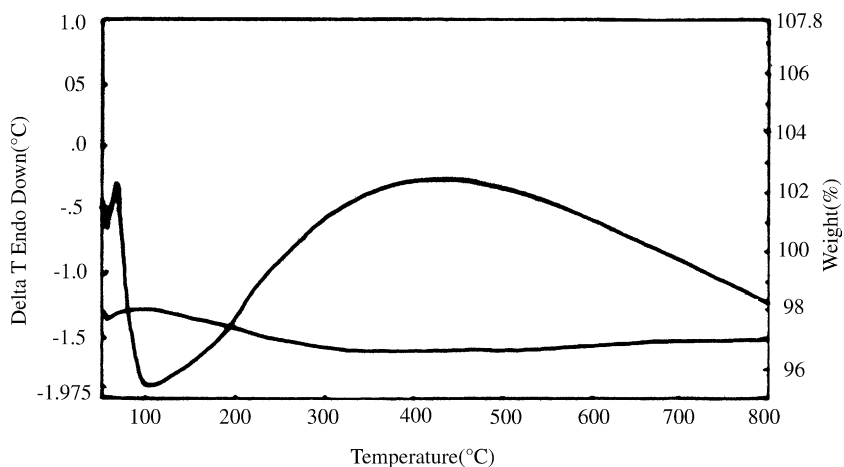


Fig. 3. TG-DTA patterns of  $\text{TiO}_2$ .

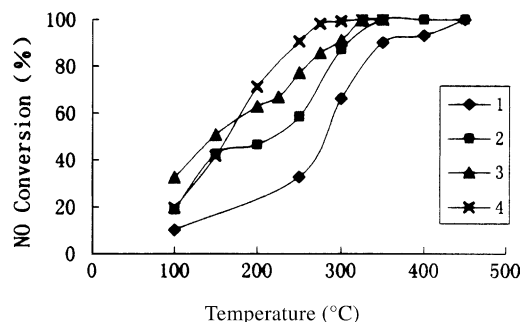


Fig. 4. Catalytic activities in NO+CO reaction under two atmospheres (1) 6% CuO/TiO<sub>2</sub> (air atmosphere); (2) 6% CuO-10% ZrO<sub>2</sub>/TiO<sub>2</sub> (air atmosphere); (3) 6% CuO/TiO<sub>2</sub> (H<sub>2</sub> atmosphere); (4) 6% CuO-10% ZrO<sub>2</sub>/TiO<sub>2</sub> (H<sub>2</sub> atmosphere).

### 3.2. Effects of CuO/TiO<sub>2</sub> and CuO-ZrO<sub>2</sub>/TiO<sub>2</sub> on NO + CO reaction

As shown in Fig. 4, the activities of 6% CuO/TiO<sub>2</sub> and 6% CuO-10% ZrO<sub>2</sub>/TiO<sub>2</sub> catalysts in H<sub>2</sub> atmosphere were much better than that in air atmosphere. The NO conversion temperature ( $T_{99\%}$ ) was 325 °C in H<sub>2</sub> and 450 °C in air for 6% CuO/TiO<sub>2</sub> catalyst. The activity order of 6% CuO-10% ZrO<sub>2</sub>/TiO<sub>2</sub> catalysts was the same as 6% CuO/TiO<sub>2</sub> in both H<sub>2</sub> and air, but  $T_{99\%}$  was 300 °C in H<sub>2</sub> and 350 °C in air. This might indicate that the addition of ZrO<sub>2</sub> increased catalytic activity in NO + CO reaction in both atmospheres.

### 3.3. Activities in NO + CO reaction by catalysts calcined at 750 and 850 °C

The activities of CuO-ZrO<sub>2</sub>/TiO<sub>2</sub> catalysts calcined at 750 °C for 2 h were similar to those calcined at 500 °C for 2 h in air atmosphere but decreased dramatically after calcination at 850 °C for 2 h (Fig. 5). The activity reduction was likely due to the fact that the heat stability of CuO could not maintain at 850 °C, which caused the gathering of active copper species. The NO conversion temperatures

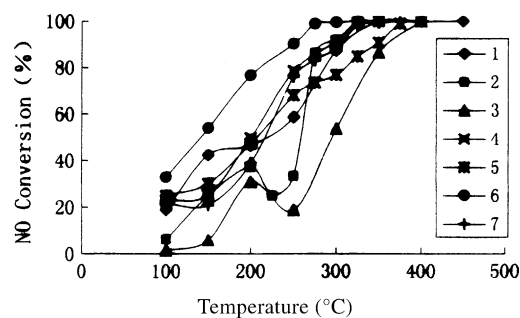


Fig. 5. NO + CO reaction by catalysts heated at 750 and 850 °C. (1) 6% CuO-10% ZrO<sub>2</sub>/TiO<sub>2</sub> (500 °C, air atmosphere); (2) 6% CuO-10% ZrO<sub>2</sub>/TiO<sub>2</sub> (750 °C, air atmosphere); (3) 6% CuO-10% ZrO<sub>2</sub>/TiO<sub>2</sub> (850 °C, air atmosphere); (4) 6% CuO-5% ZrO<sub>2</sub>/TiO<sub>2</sub> (500 °C, H<sub>2</sub> atmosphere); (5) 6% CuO-5% ZrO<sub>2</sub>/TiO<sub>2</sub> (750 °C, H<sub>2</sub> atmosphere); (6) 6% CuO-10% ZrO<sub>2</sub>/TiO<sub>2</sub> (750 °C, H<sub>2</sub> atmosphere); (7) 6% CuO-15% ZrO<sub>2</sub>/TiO<sub>2</sub> (750 °C, H<sub>2</sub> atmosphere).

( $T_{99\%}$ ) for 6% CuO-5% ZrO<sub>2</sub>/TiO<sub>2</sub> were 325 °C and 400 °C after the catalyst was calcined at 500 °C and 750 °C for 2 h in H<sub>2</sub> atmosphere, respectively.  $T_{99\%}$  was also 325 °C for 6% CuO-10% ZrO<sub>2</sub>/TiO<sub>2</sub> but increased to 350 °C for 6% CuO-15% ZrO<sub>2</sub>/TiO<sub>2</sub> after both catalysts were calcined at 750 °C for 2 h, indicating that catalytic activities decreased with increase in ZrO<sub>2</sub> loading. The findings may suggest that there was a critical amount of ZrO<sub>2</sub> loading. When 5% ZrO<sub>2</sub> was loaded, anti-high temperature property was not clear. When ZrO<sub>2</sub> loading increased to 15%, catalytic activity and heat stability decreased slightly.

### 3.4. Effect of temperature on NO, CO conversion and N<sub>2</sub> selectivity

As shown in Tables 1 and 2, the activities of 6% CuO/TiO<sub>2</sub> and 6% CuO-10% ZrO<sub>2</sub>/TiO<sub>2</sub> catalysts were better in H<sub>2</sub> than in air. NO and CO concentrations decreased simultaneously, but N<sub>2</sub> and CO<sub>2</sub> increased with increase in reaction temperatures under both atmospheres. When the catalysts were treated in air at 150 °C, the amount of N<sub>2</sub>, CO<sub>2</sub> and N<sub>2</sub>O released from NO and CO conversions increased markedly. A continuous increase in N<sub>2</sub> and CO<sub>2</sub> but a decrease in N<sub>2</sub>O was observed at 200 °C. At 300 °C, NO and CO conversions were 66.7 and 70.6% by 6% CuO/TiO<sub>2</sub> and 87.2 and 53.8% by 6% CuO-10% ZrO<sub>2</sub>/TiO<sub>2</sub>, respectively. At 350 °C, NO and CO conversions reached 99.6% by 6% CuO-10% ZrO<sub>2</sub>/TiO<sub>2</sub> compared with 91.3 and 85.6% by 6% CuO/TiO<sub>2</sub>. When the catalysts were treated in H<sub>2</sub> at 300 °C, the NO + CO reaction appeared to be complete (100%) by 6% CuO-10% ZrO<sub>2</sub>/TiO<sub>2</sub>, whereas NO and CO conversions were 91.3 and 85.5% by 6% CuO/TiO<sub>2</sub>, respectively. These results indicated that N<sub>2</sub>O was formed during the initial stage of the reaction at lower temperatures, and the amount of N<sub>2</sub>O increased with increase in temperature until a maximum of N<sub>2</sub>O was reached. Further increase in temperature, however, caused a gradual decrease in N<sub>2</sub>O until reaching zero. In contrast, the amount of N<sub>2</sub> increased continuously with increase in temperature. Therefore, it can be suggested that in the process of NO reduction with CO, the reactant molecules NO and CO were first adsorbed on the adsorption sites of catalyst surface in form of NO<sub>(a)</sub> and CO<sub>(a)</sub>, and the adsorbed NO was then dissociated into N<sub>(a)</sub> and O<sub>(a)</sub>, followed by reactions of N<sub>(a)</sub> with NO<sub>(a)</sub> and CO<sub>(a)</sub> with O<sub>(a)</sub> to produce N<sub>2</sub>O<sub>(a)</sub> and CO<sub>2</sub>, and N<sub>2</sub> formation by two N<sub>(a)</sub>. This study also shows that the rate of NO<sub>(a)</sub> dissociation on the catalyst surface was slower at low temperature and its reaction with N<sub>(a)</sub> formed N<sub>2</sub>O<sub>(a)</sub>. As the reaction temperature increased, the rate of NO<sub>(a)</sub> dissociation became faster, causing a reduction of NO<sub>(a)</sub> concentration. As a result, high temperature was not beneficial to N<sub>2</sub>O formation. Therefore, effects of the catalysts on the NO + CO reaction were not only related to the dispersion state of active components CuO on TiO<sub>2</sub> but also to the rate of NO dissociation on the catalyst surfaces.

The elementary steps involved in NO + CO reaction are widely accepted as the following equations [11], where S

Table 1  
Effect of temperature on NO, CO conversion and N<sub>2</sub> selectivity in NO + CO reaction by catalysts treated in air atmosphere

Temperature (°C)	Conversion (%)				N <sub>2</sub> Selectivity	
	6% CuO/TiO <sub>2</sub>		6% CuO-10% ZrO <sub>2</sub> /TiO <sub>2</sub>		6% CuO/TiO <sub>2</sub>	6% CuO-10% ZrO <sub>2</sub> /TiO <sub>2</sub>
	NO	CO	NO	CO		
150	30.8	21.9	42.3	21.5	13.7	0
200	35.3	21.9	46.4	25.0	10.1	9.26
250	40.9	23.0	58.5	30.2	15.9	43.9
300	66.7	70.6	87.2	53.8	65.7	91.9
350	91.3	85.5	99.6	96.3	78.4	100
400	91.8	85.2	100	99.3	100	100
450	99.0	90.2	100	100	100	100
500	100	97.3	100	100	100	100

Table 2  
Effect of temperature on NO, CO conversion and N<sub>2</sub> selectivity in NO + CO reaction by catalysts treated in H<sub>2</sub> atmosphere

Temperature (°C)	Conversion (%)				N <sub>2</sub> Selectivity	
	6% CuO/TiO <sub>2</sub>		6% CuO-10% ZrO <sub>2</sub> /TiO <sub>2</sub>		6% CuO/TiO <sub>2</sub>	6% CuO-10% ZrO <sub>2</sub> /TiO <sub>2</sub>
	NO	CO	NO	CO		
100	32.4	23.1	19.5	18.3	45.9	28.3
150	50.7	37.2	41.5	35.9	69.4	45.9
200	62.7	53.2	71.2	58.9	100	100
250	77.1	70.9	90.6	76.5	100	100
275	85.5	79.0	98.1	83.2	100	100
300	91.1	85.3	99.2	87.5	100	100
325	99.6	87.9	100	100	100	100
350	100	89.9	100	100	100	100

denotes adsorption sites of catalyst surface, and (a) denotes adsorption state,



These equations may also explain the mechanisms of thermal decomposition of NO on the 6% CuO/TiO<sub>2</sub> and 6% CuO-10% ZrO<sub>2</sub>/TiO<sub>2</sub> catalysts in this study. At low temperature, the reaction rate of steps (3) and (8) were very slow, and most of NO<sub>(a)</sub> existing on the catalyst surface formed N<sub>2</sub>O through steps (5) and (6). At high temperature, the reaction rate of step (3) was very fast and there were very few NO<sub>(a)</sub> on the catalyst surface. N<sub>2</sub>O was likely to be decomposed at high temperature, and therefore the higher reaction temperature was, the higher the selectivity of NO + CO reaction was.

### 3.5. H<sub>2</sub>-TPR of catalysts

Fig. 6 shows the TPR profiles of pure CuO, TiO<sub>2</sub>, 3% CuO/TiO<sub>2</sub> and 6% CuO/TiO<sub>2</sub> catalysts. A single peak was

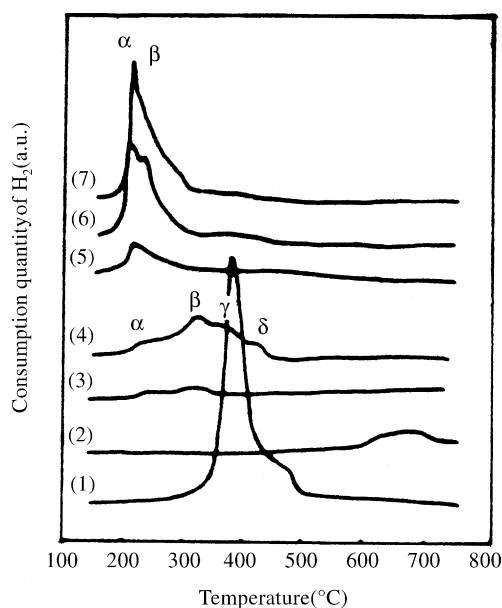


Fig. 6. TPR profiles of different catalysts. (1) CuO, (2) TiO<sub>2</sub>, (3) 3% CuO/TiO<sub>2</sub>, (4) 6% CuO/TiO<sub>2</sub>, (5) 6% CuO-5% ZrO<sub>2</sub>/TiO<sub>2</sub>, (6) 6% CuO-10% ZrO<sub>2</sub>/TiO<sub>2</sub>, (7) 6% CuO-15% ZrO<sub>2</sub>/TiO<sub>2</sub>.



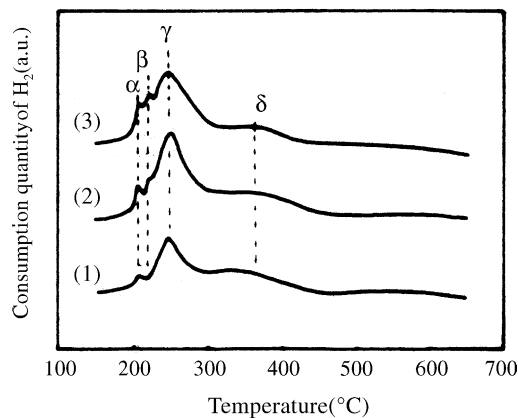


Fig. 7. TPR profiles of all catalysts calcined at 750 °C. (1) 6% CuO-5% ZrO<sub>2</sub>/TiO<sub>2</sub>, (2) 6% CuO-10% ZrO<sub>2</sub>/TiO<sub>2</sub>, (3) 6% CuO-15% ZrO<sub>2</sub>/TiO<sub>2</sub>.

observed at 392 and 650 °C for pure CuO and TiO<sub>2</sub>, respectively, indicating that TiO<sub>2</sub> reduction was very difficult. In CuO/TiO<sub>2</sub>, there were two reduction peaks (α, β) at 3% CuO loading compared with four reduction peaks (α, β, γ and δ) at 230, 325, 370 and 445 °C, respectively, when the amount of CuO loading was 6%. It was likely that the α peak resulted from the interaction of highly dispersed CuO species with TiO<sub>2</sub>, and the β peak from the oxide clusters with a structure similar to CuO, i.e. short-range order but not crystallites. The γ peak could be due to the CuO crystallites, and the δ peak due to the interactions between CuO and TiO<sub>2</sub>, and oxygen reduction on the TiO<sub>2</sub> surface [9,10].

After the addition of ZrO<sub>2</sub> into 6% CuO/TiO<sub>2</sub>, the shape and area of TPR reduction peaks increased with increase in ZrO<sub>2</sub>. Two reduction peaks (α and β) occurred in the TPR profile of 6% CuO-5% ZrO<sub>2</sub>/TiO<sub>2</sub>, with the β peak being pretty weak. When 10% ZrO<sub>2</sub> was added, both α and β peaks increased, whereas β peak disappeared at 15% ZrO<sub>2</sub> (Fig. 7). The results indicated that ZrO<sub>2</sub> might largely promote CuO dispersion on TiO<sub>2</sub>. Therefore, the cause of improvement in catalytic activities was probably related to high dispersion of

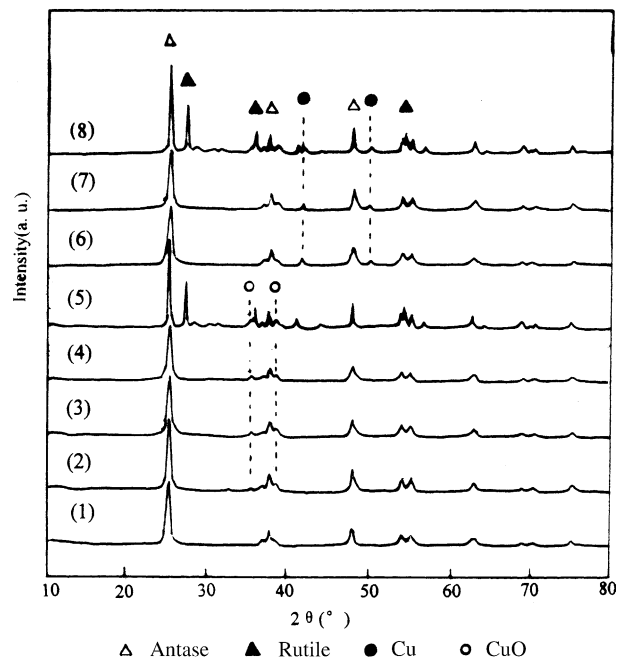


Fig. 8. XRD patterns of catalysts. (1) TiO<sub>2</sub>, (2) 6% CuO/TiO<sub>2</sub>, (3) 6% CuO-5% ZrO<sub>2</sub>/TiO<sub>2</sub>, (4) 6% CuO-15% ZrO<sub>2</sub>/TiO<sub>2</sub>, (5) 6% CuO-15% ZrO<sub>2</sub>/TiO<sub>2</sub>(750 °C), (6) 6% CuO/TiO<sub>2</sub> (500 °C, H<sub>2</sub> atmosphere), (7) 6% CuO-10% ZrO<sub>2</sub>/TiO<sub>2</sub> (500 °C, H<sub>2</sub> atmosphere), (8) 6% CuO-15% ZrO<sub>2</sub>/TiO<sub>2</sub> (750 °C, H<sub>2</sub> atmosphere).

CuO species (α peak) and fine grain CuO species (β peak). The XRD analysis also showed that addition of ZrO<sub>2</sub> into 6% CuO/TiO<sub>2</sub> did not increase the diffraction peak intensity of CuO (Fig. 8). When ZrO<sub>2</sub> loading increased to 15%, the diffraction peaks intensity of CuO remained unchanged, suggesting that highly dispersion CuO species and fine grain CuO species were the active center of NO reduction.

Fig. 7 shows the TPR profiles of CuO-ZrO<sub>2</sub>/TiO<sub>2</sub> catalysts calcined at 750 °C. There were four reduction peaks (α, β, γ and δ) in lines (1)–(3) where the ZrO<sub>2</sub> loading ranged from 5 to 15%. At 5% ZrO<sub>2</sub> loading, the δ peak was smooth and the β peak not obvious. When the amount of

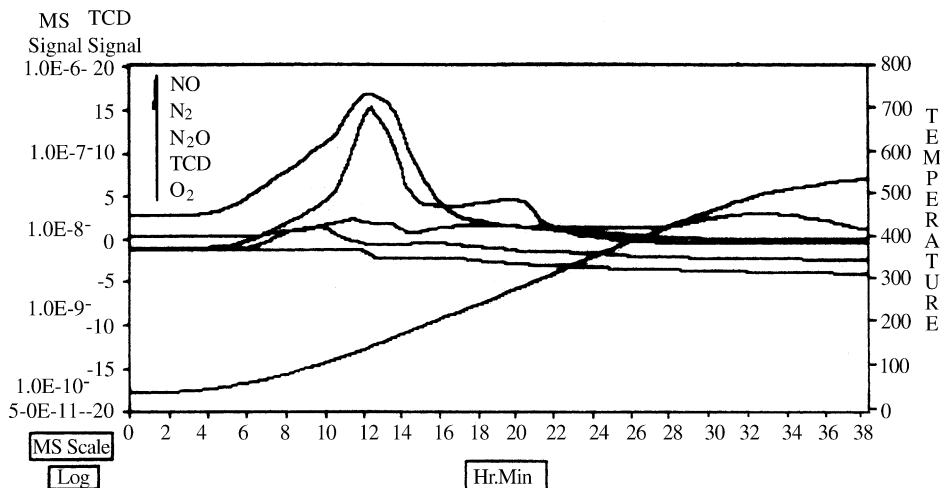


Fig. 9. NO-TPD spectra of 6% CuO/TiO<sub>2</sub> catalyst (air atmosphere) NO ( $m/e = 30$ ), N<sub>2</sub>O ( $m/e = 44$ ), N<sub>2</sub> ( $m/e = 28$ ), O<sub>2</sub> ( $m/e = 32$ ).

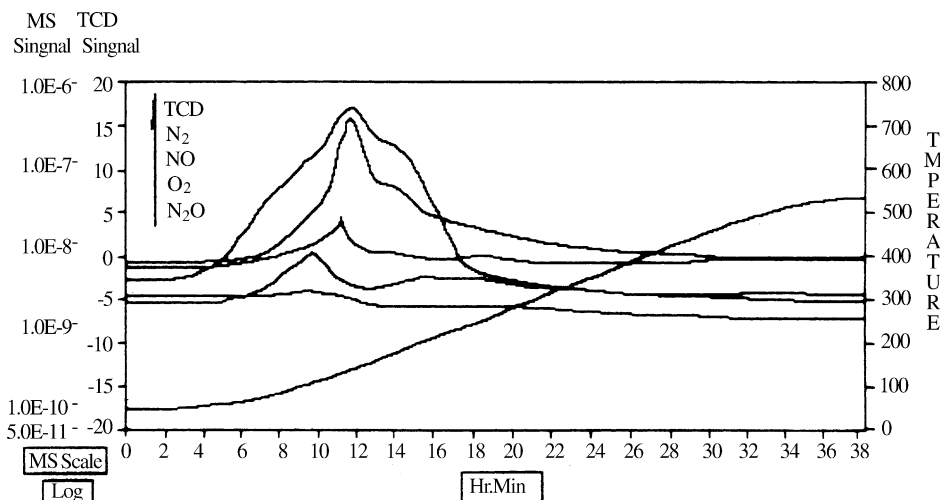


Fig. 10. NO-TPD spectra of 6% CuO-10% ZrO<sub>2</sub>/TiO<sub>2</sub> catalyst (air atmosphere) NO ( $m/e = 30$ ), N<sub>2</sub>O ( $m/e = 44$ ), N<sub>2</sub> ( $m/e = 28$ ), O<sub>2</sub> ( $m/e = 32$ ).

ZrO<sub>2</sub> loading was 10%, the  $\beta$  peak increased and the  $\alpha$  peak had small changes. With further increase in ZrO<sub>2</sub> loading, the  $\beta$  peak intensity became weaker and the shape of TPR reduction peak smoother, suggesting that the catalysts calcined at 750 °C have the same TPR profiles as those calcined at normal temperature (500 °C).

### 3.6. XRD analysis of catalysts

As shown in line (1) of Fig. 8, there was a diffraction peak of anatase at  $2\theta$ : 25.2, 37.0 and 48.1° but not a rutile phase after TiO<sub>2</sub> was calcined at 450 °C for 4 h. Two CuO diffraction peaks were obvious between  $2\theta$ , 35.5 and 38.7° plus a diffraction peak of anatase phase (line 2), indicating that the CuO on TiO<sub>2</sub> had transformed from highly dispersion CuO species to a CuO crystal phase. After addition of ZrO<sub>2</sub> (5–15%), the diffraction peak of ZrO<sub>2</sub> was not detected (lines 3 and 4) and the diffraction peak intensity of CuO did not increase either. Likely, it was the strong interac-

tion between CuO and ZrO<sub>2</sub> that enhanced the activity and stability of catalyst. XRD also detected a mixture phase of anatase and rutile after the catalysts were calcined at 750 °C for 2 h (line 5).

After 6% CuO/TiO<sub>2</sub> and 6% CuO-10% ZrO<sub>2</sub>/TiO<sub>2</sub> were pretreated at 500 °C for 1 h in H<sub>2</sub>, the CuO diffraction peaks ( $d = 2.52$  and  $2.33$ ) disappeared but Cu diffraction peaks ( $d = 2.09$  and  $1.80$ ) were detected, as shown in lines (6)–(8). By comparison, the catalysts calcined at 750 °C for 2 h in both H<sub>2</sub> and air atmospheres, the diffraction peaks of rutile ( $d = 3.25$ ,  $2.48$  and  $1.68$ ) became much stronger additional to the conversion of CuO to Cu. The results indicate that the components changed and a strong interaction took place between the CuO and ZrO<sub>2</sub>-TiO<sub>2</sub> compounds. Based on the results of this study and a previous study by Yasuaki et al. [12], we suggest that in H<sub>2</sub> atmosphere CuO produced dispersed Cu<sup>0</sup> species, and after one NO molecule on the Cu<sup>0</sup> sites formed a mononitrosyl Cu<sup>0</sup> species, another NO molecule reacted with the mononitrosyl Cu<sup>0</sup> species to pro-

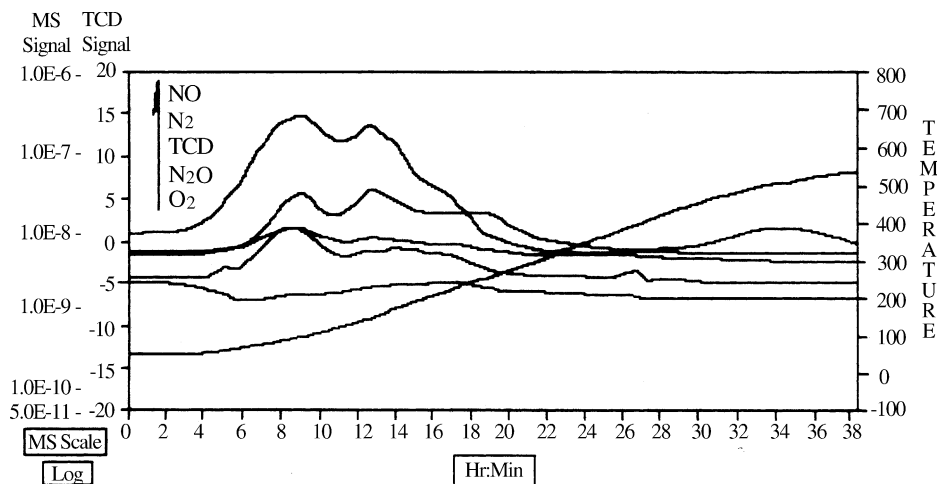


Fig. 11. NO-TPD spectra of 6% CuO/TiO<sub>2</sub> catalyst (H<sub>2</sub> atmosphere) NO ( $m/e = 30$ ), N<sub>2</sub>O ( $m/e = 44$ ), N<sub>2</sub> ( $m/e = 28$ ), O<sub>2</sub> ( $m/e = 32$ ).

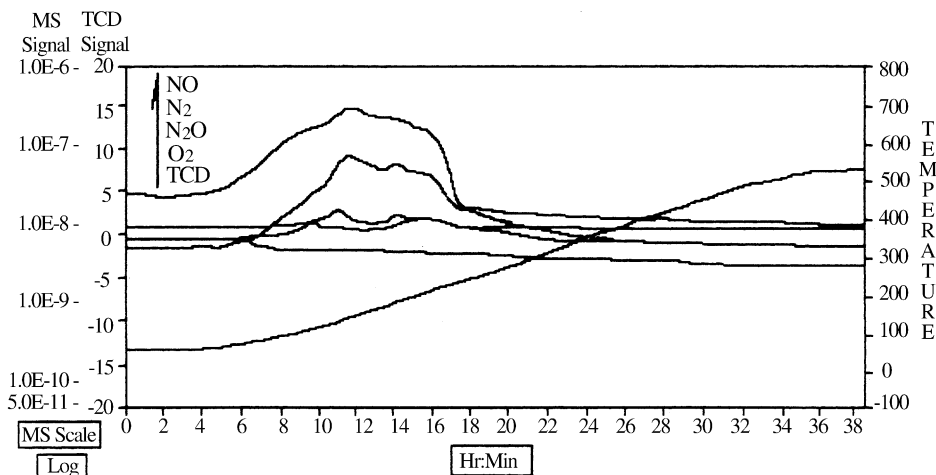


Fig. 12. NO-TPD spectra of 6% CuO-10% ZrO<sub>2</sub>/TiO<sub>2</sub> catalyst (H<sub>2</sub> atmosphere) NO ( $m/e = 30$ ), N<sub>2</sub>O ( $m/e = 44$ ), N<sub>2</sub> ( $m/e = 28$ ), O<sub>2</sub> ( $m/e = 32$ ).

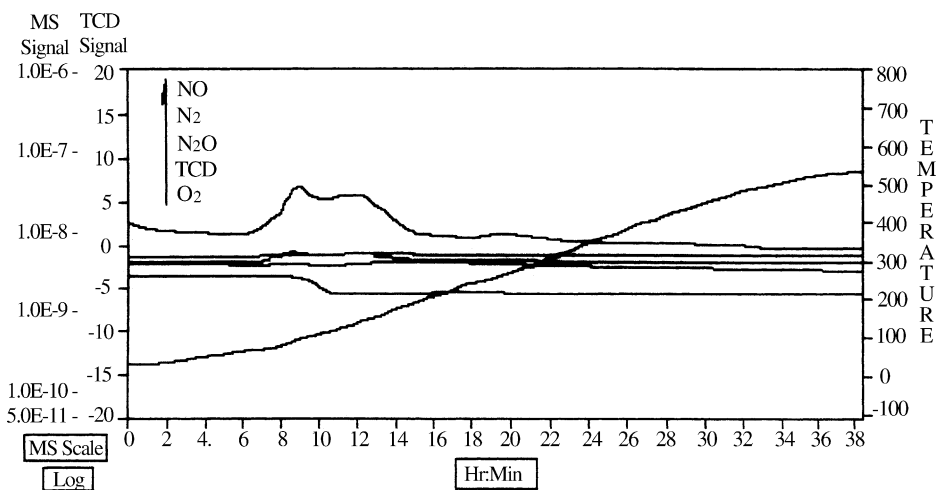


Fig. 13. NO-TPD spectra of 6% CuO/TiO<sub>2</sub> catalyst (750 °C, H<sub>2</sub> atmosphere) NO ( $m/e = 30$ ), N<sub>2</sub>O ( $m/e = 44$ ), N<sub>2</sub> ( $m/e = 28$ ), O<sub>2</sub> ( $m/e = 32$ ).

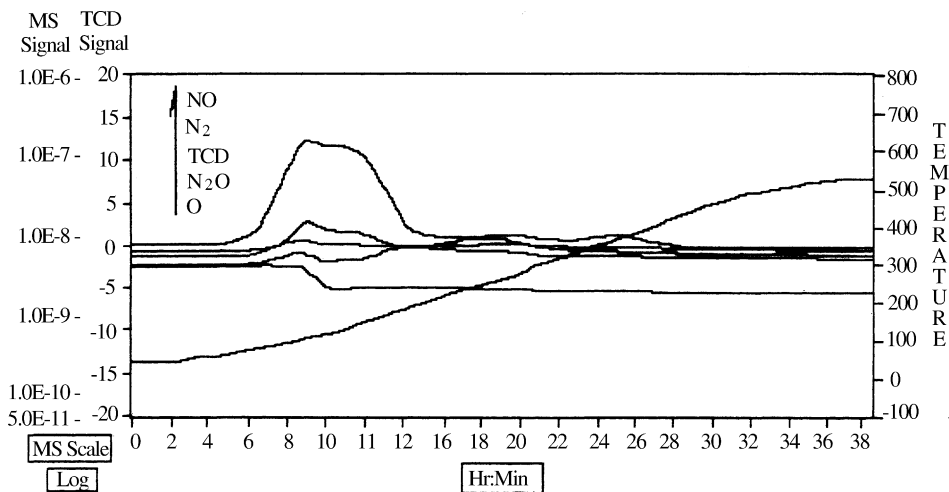


Fig. 14. NO-TPD spectra of 6% CuO-10% ZrO<sub>2</sub>/TiO<sub>2</sub> catalyst (750 °C, H<sub>2</sub> atmosphere) NO ( $m/e = 30$ ), N<sub>2</sub>O ( $m/e = 44$ ), N<sub>2</sub> ( $m/e = 28$ ), O<sub>2</sub> ( $m/e = 32$ ).



duce  $\text{N}_2\text{O}$  and an unstable dinitrosyl intermediate, and then returned back to  $\text{Cu}^0$  species, i.e. a continuous redox cycle involving  $\text{Cu}^{2+}$  and  $\text{Cu}^0$ . It was likely that NO reacted with a mononitrosyl  $\text{Cu}^0$  species to form  $\text{N}_2$  and dispersed  $\text{Cu}^0$  species.

### 3.7. NO-TPD experiment

After the surface of 6%  $\text{CuO}/\text{TiO}_2$  adsorbed NO, thermal desorption took place as a dissociation reaction, and four desorption species ( $\text{NO}$ ,  $m/e = 30$ ;  $\text{N}_2\text{O}$ ,  $m/e = 44$ ;  $\text{N}_2$ ,  $m/e = 28$  and  $\text{O}_2$ ,  $m/e = 32$ ) (Fig. 9) were detected by mass spectrometer. The NO desorption of 6%  $\text{CuO}/\text{TiO}_2$  and 6%  $\text{CuO}$ -10%  $\text{ZrO}_2/\text{TiO}_2$  pretreated in air atmosphere had three and four desorption peaks, respectively, i.e. three and four NO adsorption centers, and desorption peak temperatures were 100, 160, 200 °C, and 80, 110, 140, 180 °C, respectively. When the catalysts were pretreated in  $\text{H}_2$ , their NO desorption also had three desorption peaks, one peak due to NO adsorption on weak sites and the other two peaks due to NO adsorption on strong sites, and desorption peak temperature were 100, 150 and 220 °C, respectively. After 10%  $\text{ZrO}_2$  was added into 6%  $\text{CuO}/\text{TiO}_2$ , four NO desorption peaks occurred at 60, 100, 150 and 180 °C, indicating that NO desorption by  $\text{CuO}$ - $\text{ZrO}_2/\text{TiO}_2$  was easier than that by  $\text{CuO}/\text{TiO}_2$ . In addition, desorption peak temperature of NO by 6%  $\text{CuO}$ -10%  $\text{ZrO}_2/\text{TiO}_2$  was lower than that by 6%  $\text{CuO}/\text{TiO}_2$ , i.e. the former catalyst had higher NO dissociation activity than the latter catalyst. The two catalysts also showed  $\text{N}_2\text{O}$  desorption peak at low temperatures but  $\text{N}_2$  desorption peak at high temperatures. The NO-TPD process detected NO but not  $\text{O}_2$  desorption peak. It was likely that NO dissociation produced atomic oxygen (O) that dispersed or entered into the bulk of Cu [13,14], and the desorption of atomic oxygen could only occur at high temperatures (Figs. 10–14).

## 4. Conclusion

(1) The activities of  $\text{CuO}/\text{TiO}_2$  catalysts pre-treated in  $\text{H}_2$  were much higher than those pre-treated in air at 500 °C for 1 h. The temperatures ( $T_{99\%}$ ) of NO conversion were 325 °C in  $\text{H}_2$  and 450 °C in air. After  $\text{ZrO}_2$  was added

into  $\text{CuO}/\text{TiO}_2$ , the catalytic activities were similar to that of  $\text{CuO}/\text{TiO}_2$  in both atmospheres, i.e.  $T_{99\%}$  was 300 °C in  $\text{H}_2$  and 350 °C in air.

- (2) An addition of 5%  $\text{ZrO}_2$  into  $\text{CuO}/\text{TiO}_2$  calcined at 750 and 850 °C for 2 h caused small changes in anti-high temperature property, whereas 15%  $\text{ZrO}_2$  addition significantly increased catalytic activities, thermal stability and  $\text{N}_2$  selectivity in the  $\text{NO} + \text{CO}$  reaction.
- (3) There were four reduction peaks ( $\alpha$ ,  $\beta$ ,  $\gamma$  and  $\delta$ ) in  $\text{CuO}/\text{TiO}_2$  but only two reduction peaks in  $\text{CuO}$ - $\text{ZrO}_2/\text{TiO}_2$  at 6%  $\text{CuO}$  loading. After addition of  $\text{ZrO}_2$  into  $\text{CuO}/\text{TiO}_2$ , some change in TPR reduction peaks took place.
- (4) The catalysts pre-treated in air displayed  $\text{CuO}$  diffraction peaks, whereas those pre-treated in  $\text{H}_2$  displayed  $\text{Cu}$  diffraction peaks.
- (5) Four desorption species ( $\text{NO}$ ,  $\text{N}_2\text{O}$ ,  $\text{N}_2$  and  $\text{O}_2$ ) were produced during the thermal desorption of NO adsorbed on  $\text{CuO}/\text{TiO}_2$  and  $\text{CuO}$ - $\text{ZrO}_2/\text{TiO}_2$ . The desorption species at low temperature were the NO adsorption on weak sites and those at high temperature on strong sites. Addition of  $\text{ZrO}_2$  into  $\text{CuO}/\text{TiO}_2$  shifted the NO desorption peaks towards the low temperature range, i.e. the NO dissociation activity by  $\text{CuO}$ - $\text{ZrO}_2/\text{TiO}_2$  was higher than that by  $\text{CuO}/\text{TiO}_2$ .

## References

- [1] M. Iwamoto, H. Yahiro, Y. Mine, J. Chem. Lett. (1989) 213.
- [2] M. Iwamoto, H. Yahiro, T. Torikai, J. Chem. Lett. (1990) 1967.
- [3] D. Stoyanova, M. Christova, P. Dimitrova, Appl. Catal. B Environ. 17 (1998) 233.
- [4] G.D. Mariadasson, F. Fajardie, J. Francois, J. Mol. Catal. A Chem. 161 (2000) 179.
- [5] Y.J. Li, J.N. Armor, Appl. Catal. B Environ. 4 (1994) L1.
- [6] G. Cordaba, M. Viniegra, J. Fierro, J. Solid Chem. 138 (1998) 1.
- [7] O.V. Komova, A.V. Simakov, V.A. Rogov, J. Mol. Catal. A Chem. 161 (2000) 191.
- [8] B. Xu, D. Li, Y. Chen, Chem. Soc. Faraday Trans. 94 (1998) 1905.
- [9] P.O. Lnrsson, A. Andersson, L.R. Wallenberg, J. Catal. 163 (1996) 279.
- [10] P.O. Larsson, A. Anderson, J. Catal. 179 (1998) 72.
- [11] K.C. Byong, H.S. Brent, E.B. James, J. Catal. 115 (1989) 486.
- [12] O. Yasuaki, G. Hideki, Catal. Today 36 (1997) 71.
- [13] K.Y. Simon Ng, D.N. Belton, S.J. Schmieg, J. Catal. 146 (1994) 394.
- [14] J. Kaspar, C. Leitenburg, P. Fomasiero, J. Catal. 146 (1994) 136.